ChemComm

COMMUNICATION

View Article Online
View Journal | View Issue

Cite this: *Chem. Commun.*, 2023, 59, 6347

Received 10th March 2023,
Accepted 21st March 2023

DOI: 10.1039/d3cc01143g

rsc.li/chemcomm

Rational optimization of siRNA to ensure strand bias in the interaction with the RNA-induced silencing complex†

Dhrubajyoti Datta,[a] Christopher S. Theile,[a] Kelly Wassarman,[a] June Qin,[a] Tim Racie,[a] Karyn Schmidt,[a] Yongfeng Jiang,[a] Rachel Sigel,[a] Maja M. Janas,[a] Martin Egli[b] and Muthiah Manoharan*[a]

To ensure specificity of small interfering RNAs (siRNAs), the antisense strand must be selected by the RNA-induced silencing complex (RISC). We have previously demonstrated that a 5′-morpholino-modified nucleotide at the 5′-end of the sense strand inhibits its interaction with RISC ensuring selection of the desired antisense strand. To improve this antagonizing binding property even further, a new set of morpholino-based analogues, Mo2 and Mo3, and a piperidine analogue, Pip, were designed based on the known structure of Argonaute2, the slicer enzyme component of RISC. Sense strands of siRNAs were modified with these new analogues, and the siRNAs were evaluated *in vitro* and in mice for RNAi activity. Our data demonstrated that Mo2 is the best RISC inhibitor among the modifications tested and that it effectively mitigates sense strand-based off-target activity of siRNA.

Strand selection of small interfering RNAs (siRNAs) is a critical step in RNA interference (RNAi)-mediated gene silencing, as loading of the sense strand into the RNA-induced silencing complex (RISC) can lead to off-target effects through silencing of mRNAs complementary to this strand.[1,2] One driver of strand selection is thermodynamics: the strand with its 5′-terminus at the thermodynamically less stable end of the siRNA duplex is selected as the antisense strand.[3] Moreover, 5′-end phosphorylation is a requirement for efficient loading into the RISC.[4] Therefore, the presence of a monophosphate group or phosphate analog at the 5′-end can ensure selection of the desired strand.[5–10]

The presence of a group that blocks 5′-end phosphorylation of the sense strand also reduces off-target effects.[2,11–13] We previously reported synthesis of a 5′-morpholino modified nucleoside (**Mo1**, Fig. 1) and demonstrated that its presence at the 5′-end of the sense strand improves antisense strand selection more effectively[12] than 5′-*O*-methyl[13] or unlocked nucleic acid.[2,11] When the interaction of an siRNA with a **Mo1**-modified strand with the MID domain of Ago2 was modeled, there was not a snug fit. We reasoned that extension of the morpholino group at the point of attachment to the nucleoside 5′-end might result in a better RISC antagonist. Thus, an extended morpholino, **Mo2**, was designed and synthesized (Fig. 1). We synthesized two additional novel potential antagonists, piperidine (**Pip**) and morpholino-*N*-oxy (**Mo3**) (Fig. 1) using aminooxy click chemistry.[14]

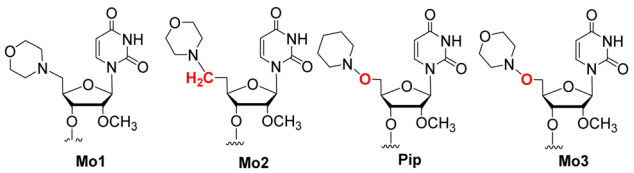

Fig. 1 Modifications investigated in this study.

Mo2 was synthesized as shown in Scheme 1. Commercially available nucleoside **1**[10] was oxidized to the aldehyde **2**[10] following the literature procedure.[15] A Wittig reaction on compound **2** produced compound **3** in good yield. Hydroboration of **3** with 9-borabicyclo[3.3.1]nonane followed by oxidation afforded compound **4** (Table S1, ESI†). The primary hydroxyl group of **4** was then tosylated to compound **5** followed by neat morpholine treatment to produce **6**. Deprotection of the *tert*-butyldimethylsilyl (TBS) group using tetrabutylammonium fluoride (TBAF) afforded **7**, which was then converted to phosphoramidite **8** by standard phosphitylation.

To synthesize the **Pip** and **Mo3** building blocks (Scheme 2), **9** was synthesized with an aminooxy (-ONH_2) group at the 5′-end of nucleoside.[14] Reductive amination of **9** with glutaraldehyde resulted in compound **10**. Removal of the TBS protecting group afforded compound **12**. Phosphitylation of **12** yielded phosphoramidite **14**. Similarly, reaction of 2-(2-oxoethoxy)acetaldehyde[16] with **9** under reductive amination conditions produced **11**, which, upon deprotection of the silyl group with TBAF, resulted in compound **13**.

[a] *Alnylam Pharmaceuticals, 675 West Kendall Street, Cambridge, Massachusetts 02142, USA. E-mail: mmanoharan@alnylam.com*
[b] *Department of Biochemistry, School of Medicine, Vanderbilt University, Nashville, Tennessee 37232, USA*

† Electronic supplementary information (ESI) available. See DOI: https://doi.org/10.1039/d3cc01143g

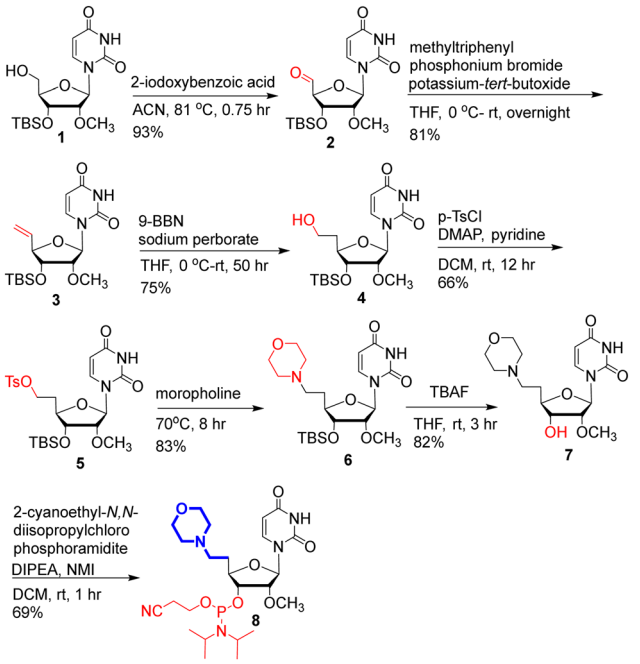

Scheme 1 Synthesis of **Mo2** phosphoramidite **8**.

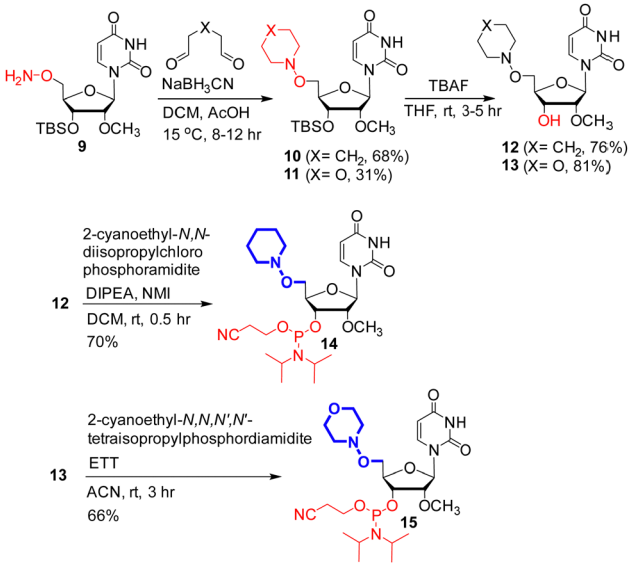

Scheme 2 Synthesis of **Pip** phosphoramidite **14** and **Mo3** phosphoramidite **15**.

Compound **13** was phosphitylated to afford the phosphoramidite **15** in moderate yield.

The modified building blocks **8**, **14**, and **15** were incorporated at the 5′-ends of oligonucleotides using standard oligonucleotide synthesis (Fig. S1, ESI†). These building blocks were used to synthesize both sense and antisense strands of siRNAs (Table S2, ESI†). In the parent siRNA, the 5′-terminal nucleotide is 2′-*O*-methyl (2′-OMe) U. We first evaluated silencing of *ApoB* expression in mice by siRNA with sense strands modified with **Mo1**, **Mo2**, **Pip**, and **Mo3** (siRNAs **I**, **III**, **IV**, and **V**, respectively, Table 1). Mice were treated

Table 1 siRNA duplexes for *in vivo ApoB* assay

Duplex	Sense strand (upper) and antisense strand (lower)[a] (5′–3′)
Parent	u•g•*UgAcAaAUAuGgGcAuCaA***L**
	u•*U*•gAu*GcCcAuauUuGuCaCa*•a•a
I	**Mo1**•g•*UgAcAaAUAuGgGcAuCaA***L**
	u•*U*•gAu*GcCcAuauUuGuCaCa*•a•a
II	u•g•*UgAcAaAUAuGgGcAuCaA***L**
	Mo1•*U*•gAu*GcCcAuauUuGuCaCa*•a•a
III	**Mo2**•g•*UgAcAaAUAuGgGcAuCaA***L**
	u•*U*•gAu*GcCcAuauUuGuCaCa*•a•a
IV	**Pip**•g•*UgAcAaAUAuGgGcAuCaA***L**
	u•*U*•gAu*GcCcAuauUuGuCaCa*•a•a
V	**Mo3**•g•*UgAcAaAUAuGgGcAuCaA***L**
	u•*U*•gAu*GcCcAuauUuGuCaCa*•a•a
VI	u•g•*UgAcAaAUAuGgGcAuCaA***L**
	Mo2•*Usg*Au*GcCcAuauUuGuCaCa*•a•a
VII	u•g•*UgAcAaAUAuGgGcAuCaA***L**
	Pip•*U*•gAu*GcCcAuauUuGuCaCa*•a•a
VIII	u•g•*UgAcAaAUAuGgGcAuCaA***L**
	Mo3•*U*•gAu*GcCcAuauUuGuCaCa*•a•a

[a] Chemical modifications are indicated as follows: •, PS linkage; lower case, 2′-OMe; italicized upper case, 2′-fluoro; **L**, trivalent-GalNAc respectively.

subcutaneously with 3 mg kg^{-1} of siRNA. The sense strands of these siRNAs were conjugated to trivalent *N*-acetylgalactosamine (Fig. S2, ESI†), to deliver siRNAs into hepatocytes after subcutaneous injection. Circulating *ApoB* protein was quantified using an ELISA assay. As previously observed,[12] we found that siRNA activity was improved compared to the parent compound when the sense strand was conjugated with **Mo1**. The duplexes with sense strands modified with **Mo2**, **Pip**, and **Mo3** had better activity than the siRNA with the **Mo1** modification (Fig. 2).

In contrast to the effects of morpholino and piperidine modifications to the sense strand, when placed at the 5′ end of the antisense strand (siRNAs **II**, **VI**, **VII**, and **VIII**, Table 1), all modifications resulted in loss of activity compared to the parent siRNA (Fig. 3). The presence of a **Mo** or **Pip** derivative likely interferes with RISC-mediated gene silencing through two mechanisms. These modifications block 5′ phosphorylation[4,17,18] and sterically interfere with effectively loading of the strand on Ago2.

To distinguish which of these modifications more effectively inhibit strand use, antisense strands targeting *TTR* were

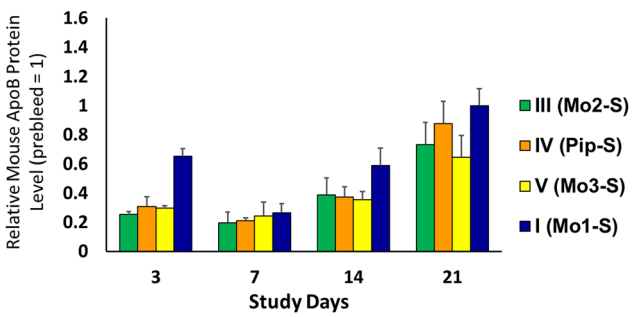

Fig. 2 Modification of the sense strand with a morpholino or piperidine derivative enhances silencing in mice. Mice (n = 3 per group) were treated with a single dose (3 mg kg^{-1}) of siRNA **I**, **III**, **IV**, or **V** targeting *ApoB*. The levels of circulating *ApoB* protein were quantified at 3, 7, 14, and 21 days. Data are expressed as fraction of *ApoB* in the PBS-treated control animals.

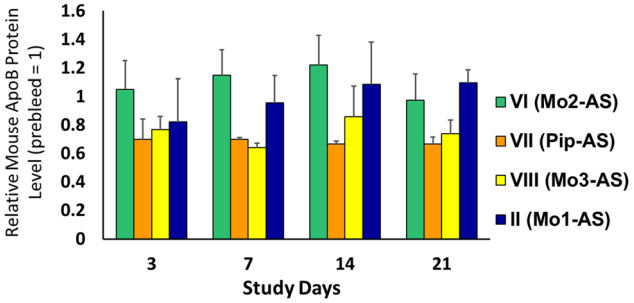

Fig. 3 **Mo1** and **Mo2** modification of antisense strands inhibit silencing. Mice (n = 3 per group) were treated with a single dose (3 mg kg^{-1}) of siRNA **II**, **VI**, **VII** and **VIII** targeting *ApoB*. The levels of circulating *ApoB* protein were quantified at 3, 7, 14, and 21 days. Data are expressed as percent of *ApoB* in the PBS-treated control animals.

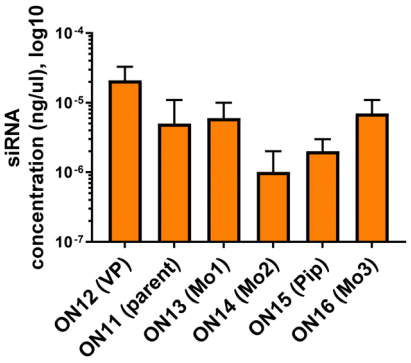

Fig. 5 **Mo2** modification at the 5′ position inhibits RISC loading. Total antisense RNA bound to recombinant human Ago2 quantified by stem-loop RT-PCR. Plotted are means ± standard deviation of three replicates.

modified with the morpholino and piperidine analogues, and siRNAs (siRNAs **IX–XII**, Table S3, ESI†) were evaluated in a previously described *in vitro* luciferase reporter assay. In this assay, the 3′ UTR of the reporter gene that encodes luciferase contains a single binding site for the antisense strand. The siRNA **X** with the **Mo2** modification was 30-fold less potent than parent (Fig. 4 and Table S3, ESI†). This resulting antagonising effect was superior to that of **Mo1**, which was 13-fold less potent than the parent siRNA. Activities of siRNAs modified with **Pip** and **Mo3** (**XI** and **XII**, respectively) were similar to that of the parent siRNA.

The residue at position 2 of the antisense strand strongly influences the stability of the complex with Ago2. Only the natural RNA, deoxy, or 2′-fluoro are tolerated at this position.[19] For example, the methyl group of the commonly used 2′-OMe sugar modification results in a steric conflict with an α-helical curl of the Ago2 MID domain.[5,6,9] Therefore, we reasoned that the RISC inhibiting ability of **Mo2** would be enhanced if we replaced the 2′-fluoro at position 2 with 2′-OMe. In the reporter assay, the siRNA with an antisense strand containing these two was inactive even at the highest dose tested (siRNA **XIII**, Table S3 and Fig. S3, ESI†). In the *in vitro* silencing assay, the modification of the sense strand with **Mo2** and a 2′-OMe at position 2 resulted in an siRNA that was active even at the lowest dose (Table S4 and Fig. S4, ESI†).

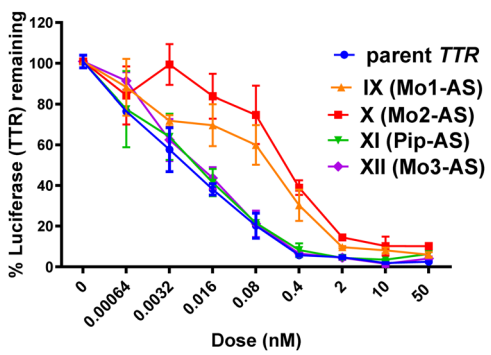

Fig. 4 Gene silencing activity is inhibited by **Mo2** modification of the antisense strand. Percent luciferase expression in *TTR* reporter assay as a function of siRNA concentration. The antisense strand of the siRNA targeting *TTR* was modified with the indicated morpholino analog. The parent strand did not have a 5′-modification.

To assess the impact of the modifications on the relative binding affinities to Ago2, the parent or morpholino-modified single strands were incubated with a commercially available recombinant human Ago2, and total RNA bound was quantified by stem-loop RT-qPCR. Significantly less oligonucleotide was loaded onto Ago2 when the 5′-position of the antisense strand was modified with **Mo2** or, to a lesser extent **Pip**, than when the antisense strand was not modified with a morpholino or when the **Mo1** modification was present (Fig. 5). The ON12 VP-modified oligonucleotide has the phosphate mimic (*E*)-vinyl phosphonate[7–10] which is known to favor MID domain binding and was used as a positive control in this experiment. (See Table S5, ESI†).

To rationalize the observation that **Mo2** more effectively inhibited use of an siRNA strand by the RNAi silencing machinery than other modifications tested, we modeled complexes between Ago2 and antisense strands containing **Mo1**, **Mo2**, **Pip**, or **Mo3** at their 5′-termini using the crystal structure of Ago2 bound to miR-20a (PDB ID 4f3t) as the starting structure.[5] All models were built using UCSF Chimera[20] and energy-minimized with Amber 14 (https://ambermd.org/)[21] as we did previously for modeling of the **Mo1**-modified strand bound to MID.[20] Multiple basic side chains are gathered around the 5′ phosphate of the antisense strand inside the Ago2 MID pocket, and interactions of **Mo2**, **Pip**, and **Mo3** docked to MID are fairly similar to those seen with **Mo1** (Fig. 6 and Fig S5 in ESI†). The **Mo2** and **Mo3** analogs, which are longer than **Mo1**, do not adopt a stretched orientation and thus are not inserted deeply into the binding pocket. These modifications are displaced by about 1 Å compared to the parent **Mo1** (Fig. S5E in ESI†). In the energy minimizations, we assigned a +1 positive charge to **Mo1** and **Mo2**, but the corresponding nitrogen was neutral in **Pip** and **Mo3**. The only H-bond acceptors or donors on the morpholinos are a nitrogen lone pair or an N–H, respectively. The latter interaction is observed in the case of **Mo2** with Tyr-529, which acts as an acceptor (Fig. S5F in ESI†). The **Mo** ring oxygen **Pip** that is a rather weak acceptor is within H-bonding distance of Lys-570 (Fig. S5 in ESI†). Interactions of the 5′ phosphate with all positively charged lysine and arginine residues as well Gln-545 are disrupted by the insertion of the 5′-**Mo** and -**Pip** modifications. Compared to **Mo1**, the slightly longer **Mo2**, **Pip**, and **Mo3** modifications have even more unfavorable steric interactions with these basic side chains (Fig. S5E in ESI†). For

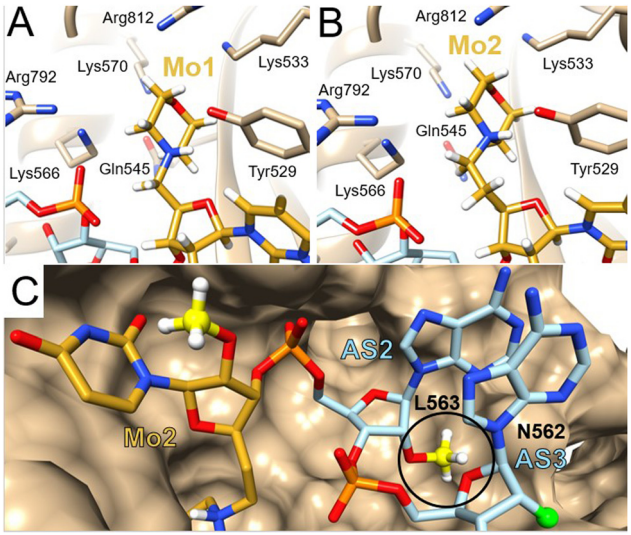

Fig. 6 Morpholino analogues disrupt interaction of the 5′-phosphate with the MID domain of Ago2. Models of Ago2 bound to strands with (A) **Mo1**,[20] and (B) **Mo2**, (C) Model of the complex with Mo2 and 2′-OMe at the first and second positions (AS1 and AS2, respectively). The 2′-OMe at AS2 slightly penetrates the Ago2 surface and clashes with N562 (solid circle). 2′-OMe is highlighted in ball-and-stick mode with carbon and hydrogen atoms colored in yellow and white, respectively. The 2′-F at AS3 is shown as a green sphere.

example, Lys-533 has its NH_3^+ headgroup turned away and presents a methylene in the direction of **Mo** and **Pip** moieties in complexes with strands with the longer modifications (Fig. 6 and Fig. S5E in ESI†). All morpholino groups are electrostatically incompatible with the MID domain binding site (Fig. S5 in the ESI†). Thus, **Mo2** incorporated at the 5′-end of the strand appears to be more disruptive than **Mo1** as observed experimentally. Further, modeling indicates that the combination of **Mo2** with 2′-OMe results in multiple steric clashes within the binding site for the antisense strand within Ago2 (Fig. 6C).

In conclusion, three phosphoramidite building blocks were synthesized to allow incorporation of extended morpholino or piperidine functional groups at the 5′-position of oligonucleotides. In mice, in a reporter gene assay, and in an assay to monitor loading onto RISC, the **Mo2** modification most effectively inhibited loading of an siRNA strand of the modifications tested. This extended morpholino derivative should mitigate previously described sense strand-mediated off-target effects[22–25] and will be useful for studies of ascertaining the role of the antisense strand in downstream RNAi mediated side-effects if any, by blocking the antisense strand using this chemistry.[26] These modifications are also expected to improve resistance to degradation by 5′-exonucleases. In this context, the combination of **Mo2** with 2′-OMe at AS2 functions as the effective antisense blocker (Fig. 6C). When used in sense strands, the **Mo2** modification should enhance potency and specificity by inhibiting use of this strand by blocking 5′-phosphorylation and by sterically hindering interaction with Ago2. In summary, the modifications evaluated here have the potential of improving the efficacy and safety of RNAi therapeutics and deserve further evaluation.[27]

Author contributions: The manuscript was written through contributions of all authors. All authors contributed to the design, execution of experiments, interpretation and writing of the manuscript and ESI.†

Conflicts of interest

All the authors except ME are employees of Alnylam Pharmaceuticals.

Notes and references

1 N. M. Snead, J. R. Escamilla-Powers, J. J. Rossi and A. P. McCaffrey, *Mol. Ther.–Nucleic Acids*, 2013, **2**, E103/101–E103/106.
2 N. Vaish, F. Chen, S. Seth, K. Fosnaugh, Y. Liu, R. Adami, T. Brown, Y. Chen, P. Harvie, R. Johns, G. Severson, B. Granger, P. Charmley, M. Houston, M. V. Templin and B. Polisky, *Nucleic Acids Res.*, 2011, **39**, 1823–1832.
3 D. S. Schwarz, G. Hutvagner, T. Du, Z. Xu, N. Aronin and P. D. Zamore, *Cell*, 2003, **115**, 199–208.
4 S. Weitzer and J. Martinez, *Nature*, 2007, **447**, 222–226.
5 E. Elkayam, C.-D. Kuhn, A. Tocilj, A. D. Haase, E. M. Greene, G. J. Hannon and L. Joshua-Tor, *Cell*, 2012, **150**, 100–110.
6 N. T. Schirle and I. J. MacRae, *Science*, 2012, **336**, 1037–1040.
7 T. P. Prakash, W. F. Lima, H. M. Murray, W. Li, G. A. Kinberger, A. E. Chappell, H. Gaus, P. P. Seth, B. Bhat, S. T. Crooke and E. E. Swayze, *Nucleic Acids Res.*, 2015, **43**, 2993–3011.
8 N. T. Schirle, G. A. Kinberger, H. F. Murray, W. F. Lima, T. P. Prakash and I. J. MacRae, *J. Am. Chem. Soc.*, 2016, **138**, 8694–8697.
9 E. Elkayam, R. Parmar, C. R. Brown, J. L. Willoughby, C. S. Theile, M. Manoharan and L. Joshua-Tor, *Nucleic Acids Res.*, 2017, **45**, 3528–3536.
10 R. G. Parmar, C. R. Brown, S. Matsuda, J. L. S. Willoughby, C. S. Theile, K. Charisse, D. J. Foster, I. Zlatev, V. Jadhav, M. A. Maier, M. Egli, M. Manoharan and K. G. Rajeev, *J. Med. Chem.*, 2018, **61**, 734–744.
11 N. M. Snead, J. R. Escamilla-Powers, J. J. Rossi and A. P. McCaffrey, *Mol. Ther.–Nucleic Acids*, 2013, **2**, E103/101.
12 P. Kumar, R. G. Parmar, C. R. Brown, J. L. S. Willoughby, D. J. Foster, I. R. Babu, S. Schofield, V. Jadhav, K. Charisse, J. K. Nair, K. G. Rajeev, M. A. Maier, M. Egli and M. Manoharan, *Chem. Commun.*, 2019, **55**, 5139–5142.
13 P. Y. Chen, L. Weinmann, D. Gaidatzis, Y. Pei, M. Zavolan, T. Tuschl and G. Meister, *RNA*, 2008, **14**, 263–274.
14 D. Datta, S. Mori, M. Madaoui, K. Wassarman, I. Zlatev and M. Manoharan, *Org. Lett.*, 2022, **24**, 4496–4501.
15 M. J. Fer, P. Doan, T. Prange, S. Calvet-Vitale and C. Gravier-Pelletier, *J. Org. Chem.*, 2014, **79**, 7758–7765.
16 M. Israel and R. J. Murray, *J. Med. Chem.*, 1982, **25**, 24–28.
17 C.-D. Kuhn and L. Joshua-Tor, *Trends Biochem. Sci.*, 2013, **38**, 263–271.
18 N. H. Tolia and L. Joshua-Tor, *Nat. Chem. Biol.*, 2007, **3**, 36–43.
19 M. Egli and M. Manoharan, *Acc. Chem. Res.*, 2019, **52**, 1036–1047.
20 E. F. Pettersen, T. D. Goddard, C. C. Huang, G. S. Couch, D. M. Greenblatt, E. C. Meng and T. E. Ferrin, *J. Comput. Chem.*, 2004, **25**, 1605–1612.
21 D. A. Case, T. E. Cheatham Iii, T. Darden, H. Gohlke, R. Luo, K. M. Merz Jr, A. Onufriev, C. Simmerling, B. Wang and R. J. Woods, *J. Comput. Chem.*, 2005, **26**, 1668–1688.
22 K. Yoshikawa, A. Ogata, C. Matsuda, M. Kohara, H. Iba, Y. Kitade and Y. Ueno, *Bioconjugate Chem.*, 2011, **22**, 42–49.
23 T. Kubo, K. Yanagihara, Y. Takei, K. Mihara, Y. Sato and T. Seyama, *Biochem. Biophys. Res. Commun.*, 2012, **426**, 571–577.
24 Y. Kamiya, J. Takai, H. Ito, K. Murayama, H. Kashida and H. Asanuma, *ChemBioChem*, 2014, **15**, 2549–2555.
25 V. Kotikam and E. Rozners, *Acc. Chem. Res.*, 2020, **53**, 1782–1790.
26 M. M. Janas, M. K. Schlegel, C. E. Harbison, V. O. Yilmaz, Y. Jiang, R. Parmar, I. Zlatev, A. Castoreno, H. Xu, S. Shulga-Morskaya, K. G. Rajeev, M. Manoharan, N. D. Keirstead, M. A. Maier and V. Jadhav, *Nat. Commun.*, 2018, **9**, 1–10.
27 M. Egli and M. Manoharan, *Nucleic Acids Res.*, 2023, gkad067.

